A new listing of the effective r_s values for metals

A new listing of the effective r_s values for metals

F Perrot† and M Rasolt‡§

† Centre d'Etudes de Limeil-Valenton, 94195 Villeneuve St Georges Cédex, France
‡ Solid State Division, Oak Ridge National Laboratory, Oak Ridge, TN 37831-6032, USA

Abstract. Using concepts from density functional theory, we provide a list of values for the effective free-electron density paramter r_s in simple and 3d, 4d and 5d transition metals, which satisfy a necessary condition appropriate for correctly describing ground state properties of arbitrary defects in these systems. As an application, we plot the surface energy γ of these metals versus the r_s determined. A very clear correlation between γ and r_s is observed, except for the magnetic metals. This list should, therefore, replace the much more *ad hoc* estimate of the r_s values used previously.

1. Introduction

Even though considerable progress has been made over the last twenty years in treating the full many-body ground state of a highly non-uniform (and sometimes, as a direct consequence, strongly correlated) electron fluid *as a whole*, wide interest does remain in separating and defining the response of the 'free' mobile part of the electron fluid using an *effective* r_s of a uniform electron gas. This interest remains particularly in systems with low symmetry. In view of recent renewed interest in properties of electron fluids in the presence of a strong external magnetic field, which immediately reduces the symmetry of the system, this concept of an effective r_s deserves further consideration. With this in mind, we report a unique list of such r_s values, which we believe satisfy a necessary condition to appropriately describe the ground state properties of the mobile part of the electron fluid in the 3d, 4d and 5d series. We also show that our definition makes sense in the case of simple metals. These values can therefore serve a useful starting point in such low-symmetry problems.

In section 2, we describe the model used for calculating r_s in a given metal. The numerical results are presented and discussed in section 3. Finally, several additional observations are made together with our conclusion in the last section.

2. Method for extracting the r_s value in a metal

The Hamiltonian H of a many-electron system in the second quantized representation is [1]:

$$H = \int dr \left\{ -\frac{h^2}{2m} \psi^+(r) \Delta \psi(r) + [V(r) + U(r)] \psi^+(r) \psi(r) \right\}$$

$$+ \frac{1}{2} \int dr\, dr'\, v\left(|r - r'|\right) \psi^+(r) \psi(r) \psi^+(r') \psi(r') \tag{1}$$

§ Deceased.
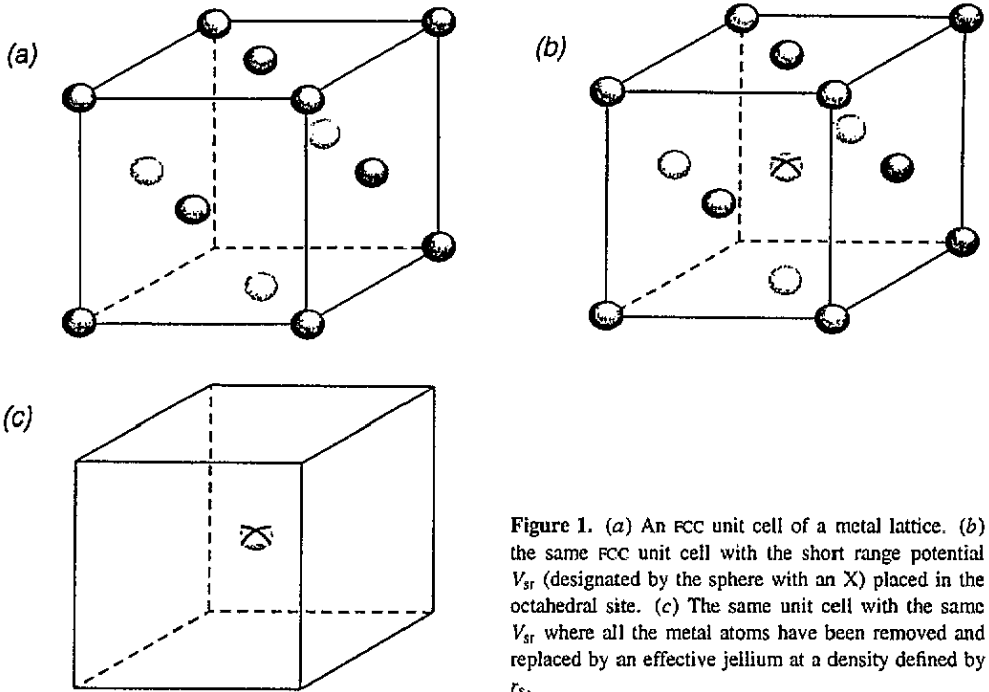
Figure 1. (a) An FCC unit cell of a metal lattice. (b) the same FCC unit cell with the short range potential V_{sr} (designated by the sphere with an X) placed in the octahedral site. (c) The same unit cell with the same V_{sr} where all the metal atoms have been removed and replaced by an effective jellium at a density defined by r_s.

where $v(|r - r'|) = e^2/|r - r'|$, $V(r)$ is the periodic part of the external potential and $U(r)$ is the part of an external potential with arbitrary symmetry, such as vacancies, interstitials, dislocations, and cleaved surfaces. The presence of an external magnetic field introduces an external gauge field [2], which further reduces the symmetry of H. Although its perturbation on the periodic part of H is a little different (i.e., it breaks the time reversal symmetry [2]), for the purpose of this derivation, it can be assumed to be part of $U(r)$.

Now H with a general $V(r)$ (ignoring the quartic term) produces a spectrum of 'bound' (or localized) bands and 'free' (delocalized) bands, but the quartic term correlates this spectrum within the bands and even more importantly between the bands. Therefore, how can we provide a necessary condition for the definition (*if there is one*) for this free electron r_s? This difficulty is perhaps best illustrated by an idealized form of (1) (the Anderson lattice Hamiltonian) given by [3]

$$\mathcal{H} = \sum_{k,\alpha,\sigma} \epsilon_{k\alpha} c^+_{k\alpha\sigma} c_{k\alpha\sigma} + E_1 \sum_{i\beta\sigma} d^+_{i\beta\sigma} d_{i\beta\sigma} + \sum_{k,\alpha,i,\beta,\sigma} (V_{k\alpha\beta} d^+_{i\beta\sigma} c_{k\alpha\sigma} \exp(i k \cdot r_i) + \text{cc})$$

$$+ \frac{U}{2} \sum_{i,(\beta,\sigma)\neq(\beta',\sigma')} N_{di\beta\sigma} N_{di\beta'\sigma'} \tag{2}$$

where the first and second terms are the free and localized contributions independently with dispersions $\epsilon_{k\alpha}$ and a single bound level E_1, respectively. The index β runs over the 3d, 4d or 5d manifold with two spins σ and α runs over the conduction band index. The third term hybridizes the free band and localized d levels and the fourth term is the Hubbard repulsion. These last two terms in (2) make the separation between free electrons and localized electrons rigorously impossible.

We now describe our procedure for generating a unique set of r_s values, which we believe are far superior (at least for ground state properties) to the existing standard listings [4, 5].

Let us look for example at FCC copper. As a first step (see figure 1(a)) we calculate the self-consistent band structure density $n_c(r)$ throughout the FCC unit cell using the density functional theory structure for the exchange and correlation potential v_{xc}. As is well known, if this v_{xc} were known exactly (it is not), then this would give rigorously $n_c(r)$ for (1). Practically, we use a standard augmented plane wave (APW) programme for two-component systems, with muffin tin spheres for the copper atoms and empty muffin tin spheres at the octahedral sites. As a second step we introduce a periodic test potential $V_{sr}(r)$ at the octahedral site of each FCC unit cell (see figure 1(b)) with $V_{sr}(r)$ in each site given by

$$V_{sr}(r) = \begin{cases} -\lambda Z_1 \left(\dfrac{1}{r} - \dfrac{1}{r_0} \right) & \text{for } r < r_0 = 1 \text{ a.u.} \\ 0 & \text{for } r < r_0 \end{cases} \tag{3}$$

where $0 < \lambda \leqslant 1$ and $Z_1 = 1$ (this choice of $V_{sr}(r)$ is discussed below). We again solve for a new density $n_c(r) + \Delta n(r)$, where $\Delta n(r)$ is the change due to $V_{sr}(r)$.
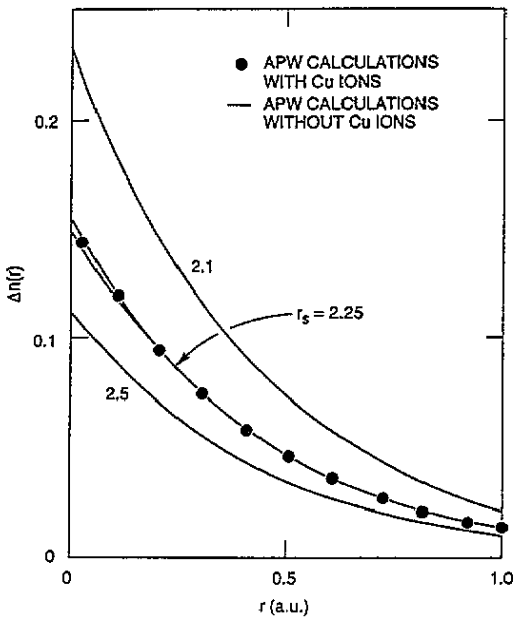

Figure 2. Calculation of the displaced densities due to V_{sr} in copper. The solid dots are the displaced densities $\Delta n(r)$ when V_{sr} is placed in the copper lattice as illustrated in figure 1(b). The solid curves are the displaced densities $\Delta n_0(r)$ when V_{sr} is placed in various jellium backgrounds as illustrated in figure 1(c). The closest fit (i.e., smallest σ) occurs when $r_s = 2.25$.
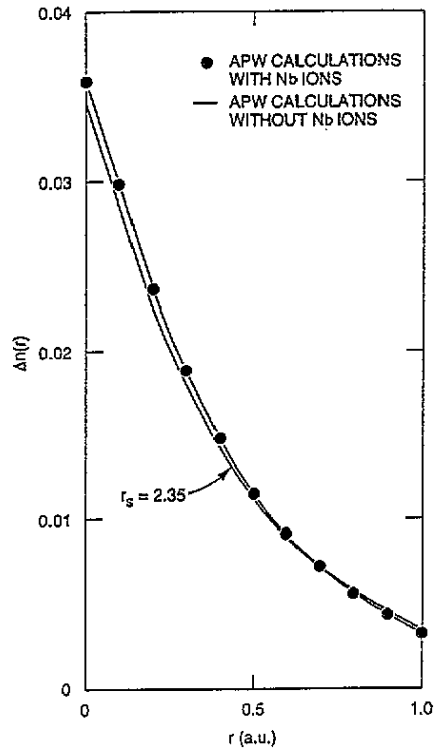
Figure 3. As figure 2, but for niobium.

Before we turn to the third step we first give a precise definition of r_s: it is the density parameter of the uniform jellium with density number $= (\frac{4}{3}\pi r_s^3)^{-1}$, which as closely as

possible replaces (1), when the ground state properties of the virgin lattice ($U(r) = 0$) are perturbed by a finite $U(r)$. Therefore, as a third step we set $V(r) = 0$ in (1) and leave the same periodic structure of the $V_{sr}(r)$ alone now, in a jellium background (figure 1(c)). We then solve again for the induced density $\Delta n_0(r)$ over a range of r_s, and search for the r_s value for which $\Delta n_0(r)$ best reproduced $\Delta n(r)$ (see figure 2 and 3).

It is obvious that our values of r_s satisfy a necessary condition in accordance with the above definition of r_s. However, this clearly does not imply that other properties, such as optical properties, have been properly replaced (or can ever be replaced) by such a concept. In fact, it is not even clear to what accuracy ground state properties of a defect of general symmetry (e.g., $U(r)$ corresponding to a cleaved metal surface of niobium) are represented by such an effective r_s. Therefore, by a necessary condition, we mean that if there exists an r_s valid for a general defect of arbitrary symmetry, it must be given by our procedure. Actually there is a little more in this procedure than first meets the eye. Again we write

$$n(r) = n_c(r) + \Delta n(r)$$

where $\Delta n(r)$ is the density displaced by $U(r)$ of (1) and $n_c(r)$ is the unrelaxed density of the perfect metal. Assume next that $U(r)$ is spherically symmetric and we scale it to $\lambda U(r)$. Via the Hellman–Feynman theorem, if $\Delta n_\lambda(r)$ is the density displaced by $\lambda U(r)$, then the energy is

$$E(n_c + \Delta n) = E(n_c) + \int_0^1 U \cdot (n_c + \Delta n_\lambda)\, d\lambda \tag{4}$$

where we use the notation

$$f \cdot g = \int f(r)g(r)\, dr. \tag{5}$$

According to (4) and (5), the main task of calculating E is obtaining the quantity $\Delta n_\lambda(r)$ for the whole range of $0 \leqslant \lambda \leqslant 1$. In fact, from (4) (even though the underlying density $n_c(r)$ is non-spherical) only the spherical component of $\Delta n_\lambda r$) is required when $U(r)$ is spherical. Of course the density $n_c(r)$ governs $\Delta n_\lambda(r)$ and leads through our above procedure to the appropriate r_s. However, once the appropriate jellium is defined, the calculation of the ground state energy follows directly from the jellium model with the effective r_s. There is an additional contribution from the unrelaxed density $n_c(r)$ (i.e., $U \cdot n_c$ in (4)) but that is trivial to calculate. In short, there is no 'non-linear' coupling between $n_c(r)$ and $\Delta n_0(r)$, and the ground state properties of the defected lattice can be calculated using the density response entirely within the jellium model with an appropriate r_s. If $U(r)$ has arbitrary symmetry, then $U(r) = \sum V_{lm}(r)Y_{lm}(\Omega)$ and, again according to the Hellman–Feynman theorem, the ground state energy can be calculated entirely using the density response of the jellium to $U(r)$.

3. Results and discussion

3.1. Alkali metals

We first look at the results in table 1 for alkali metals. Our values are $r_s = 3.13, 3.68, 4.21,$ 4.46 and 5.01 for Li, Na, K, Rb and Cs. These results are different from the 'standard' values r_{s0} obtained for monovalent metals with a fully delocalized density, which are

Table 1. Values of the free electron density parameter of metals: upper rows r_s determined in the present work; lower rows, r_s^* determined from the interstitial density obtained in the KKR calculations of [6] (data exist for $Z < 50$ only).

Li	Be								
3.13	1.86								
3.07	1.85								
Na	Mg	Al							
3.68	2.78	2.42							
3.67	2.58	2.12							
K	Ca	Sc	Ti	V	Cr	Mn	Fe	Co	Ni
4.21	3.07	2.58	2.23	2.12	2.05	2.04	2.06	2.08	2.14
4.37	2.96	2.33	2.00	1.80	1.71	1.70	1.71	1.74	1.83
Cu	Zn	Ga							
2.25	2.49	2.51							
1.95	2.11	2.28							
Rb	Sr	Y	Zr	Nb	Mo	Tc	Ru	Rh	Pd
4.46	3.34	2.69	2.44	2.35	2.23	2.21	2.23	2.29	2.39
4.68	3.16	2.44	2.08	1.91	1.77	1.77	1.79	1.86	2.02
Ag	Cd	In	Sn	Sb					
2.61	2.91	2.85	2.98	3.33					
2.23	2.44	2.57	—	—					
Cs	Ba	La	Hf	Ta	W	Re	Os	Ir	Pt
5.01	3.24	2.89	2.47	2.36	2.27	2.21	2.21	2.26	2.37
—	—	—	—	—	—	—	—	—	—
Au	Hg	Tl	Pb	Bi					
2.54	2.90	3.04	3.11	3.48					
—	—	—	—	—					

$r_{s0} = 3.16, 3.79, 4.65, 5.03$ and 5.75 respectively. In each case, $r_s < r_{s0}$. This implies that the Fermi energy (k_F) associated with r_s should be

$$k_F^2/2m = \epsilon_F = k_{F0}^2/2m^* \tag{6}$$

where k_{F0} corresponds to the standard r_{s0} and m^* is the band structure effective mass. The relation

$$k_F = k_{F0}/\sqrt{m^*} \tag{7}$$

is approximately satisfied with accepted values of m^* for Na, K, Rb and Cs, but not for Li which, with $m^* > 1$, should have $r_s > r_{s0}$. In fact, our r_s value is not determined by (6), but from an adjustment of charge densities. Using linear response for alkali metals, we can write that the density profile $\Delta n(r)$ is

$$\Delta n(r) = -\frac{1}{\pi^2} \frac{m^* k_{F0}}{\Omega} \sum_K \frac{K^2 f(K/2k_{F0})}{K^2 + (4/\pi)m^* k_{F0} f(K/2k_{F0})} V_{sr}(K) \exp(\mathrm{i}K \cdot r) \tag{8}$$

where the function $f(x)$ is that associated with the Lindhard response function

$$f(x) = \tfrac{1}{2} + [(1 - x^2)/4x] \ln |(1 + x)/(1 - x)|$$

Table 2. Classification of the metals according to the accuracy of the fit of $\Delta n(r)$ with the density $\Delta n_0(r)$ displaced in a jellium with an effective r_s. σ is the mean square difference between $\Delta n(r)$ and $\Delta n_0(r)$, (9) in the text.

$100\sigma < 0.5$	$0.5 \leqslant 100\sigma < 1$	$1 \leqslant 100\sigma < 5$	$5 \leqslant 100\sigma$
Li			Be
		Na, Mg, Al	
Cu	Ni, Zn	K, Ca, Sc, Ti, V, Cr, Mn, Fe, Co	Ga
	Tc, Cd	Rb, Sr, Zr, Mo, Ru, Rh, Ag, Sn, Sb	Y, Nb, Pd, In
	Ba, Os	Cs, La, Hf, W, Re, Ir, Pt, Au, Hg, Pb, Bi	Ta, Tl

K is a reciprocal lattice vector, Ω the atomic volume and $V_{sr}(q)$ the Fourier transform of the test potential. The local field correction has been omitted for simplicity in (8). In our procedure, we search the best fit of this charge density with the following expression:

$$\Delta n_0(r) = -\frac{1}{\pi^2} \frac{k_F}{\Omega} \sum_K \frac{K^2 f(K/2k_F)}{K^2 + (4/\pi)k_F f(K/2k_F)} V_{sr}(K) \exp(iK \cdot r)$$

by adjusting k_F (i.e. R_s). Note that there is no effective mass in the latter expression. Thus the relation of our r_s to k_{F0} and m^* is much more involved than (6), and this explains the result for Li.

In table 1, we also show the r_s^* values computed by Moruzzi *et al* for Li, Na, K and Rb from the average electron density in the interstitial region (outside the muffin tin spheres) that they obtained in their Korringa–Kohn–Rostoker (KKR) band structure calculations [6]. We see that, again with an exception for Li, these values are intermediate between ours and the 'standard' values r_{s0}.

3.2. Other metals

Our r_s values for the other simple metals and the 3d, 4d and 5d transition metals are shown in table 1. We also report for comparison the r_s^* values of Moruzzi *et al*, which are published for $Z < 50$ [6]. The common situation is that the r_s obtained using the present procedure is larger than the r_s^* obtained from the KKR interstitial average density n_{out}. This is easily explained noting that, except in alkali metals, the d electrons contribute to this density n_{out} because they extend farther than the muffin tin radius, but they do not contribute significantly in the metal response to the test potential V_{sr} because they are too rigid.

In table 2 we show a classification of the metals according to the accuracy of the fit of $\Delta n(r)$ by the density $\Delta n_0(r)$ of the effective jellium, inside the sphere of radius $r_0 = 1$ au (in the octahedral site of the metal). The spherical parts of the densities are compared for $N = 11$ values r_i of the radius in the sphere, and a mean square relative deviation σ is calculated:

$$\sigma^2 = \frac{1}{N} \sum_{r_i} \left(1 - \frac{\Delta n_0(r_i)}{\Delta n(r_i)}\right)^2. \tag{9}$$

The optimum value of r_s is the value that minimizes σ. The fit is most accurate in lithium and copper. It is rather poor in several transition metals and also in beryllium (probably due to the band structure effects in the metal) and gallium.

3.3. Application to the analysis of the surface energy

It would be interesting to see how the r_s values given in table 1 correlate with properties involving the response of the metals to a low-symmetry perturbation. Obviously, the experimental data associated with such properties must be known for all the metals studied here in order to allow a systematic comparison. The surface energy γ is a good candidate for this study because a complete list of the experimental values is available [7]. Unfortunately, the early work of Lang and Kohn [8] has shown that the jellium model does not reproduce the surface energy γ of *simple metals* with $r_s < 4$. Including discrete ionic pseudopotentials as a *first-order perturbation* was shown to be crucial for bringing the results into quantitative agreement with experiment. This does not mean that the surface electron density $\Delta n(r)$ of the jellium is inadequate for treating the surface properties: the discrete nature of the ions is necessary only for a correct estimate of the electrostatic energy (the cleavage energy, for instance, vanishes in the uniform background model). Thus the jellium approximation may still be considered as a valuable approximation for generating the electron density provided that the total surface energy properly includes the electrostatic perturbation due to the lattice of ions.

In order to overcome this difficulty of the first-principles approach, which does not relate γ to r_s straightforwardly, we take advantage of the phenomenological model of metal surfaces proposed by Kohn and Yaniv [9]. Their analysis relates the surface energy γ to the reversible cleavage force $F(x)$ required to split the metal in two pieces. They show that

$$\gamma = \alpha(AC)^{1/2} \tag{10}$$

where α is a constant for similar materials, and A and C are force constants. The force $F(x)$ goes at short distances like Ax and, at large distances, like C/x^3 (x is a scaled distance). In a simple metal, C is proportional to the plasma frequency $\omega_p = (4\pi n e^2)^{1/2}$, so it depends on r_s only. A is related to the longitudinal phonon frequencies and, as suggested by March and Tosi [10], can be approximated by $(aK)^{-1}$, with a the average interatomic distance and K the compressibility. As K is itself strongly correlated to r_s (see [6]), one arrives at

$$\gamma = (Z^*)^{-1/6}\Gamma(r_s) \tag{11}$$

valid in a simple metal, with $\Gamma(r_s)$ an unexplicited function of r_s. Neglecting the weak dependence of γ on $Z^*((Z^*)^{1/6}$ varies from 1 to 1.16 for all the metals of table 1), we will see whether γ correlates with the effective r_s in any metal. Let us also note that, in (11), γ is an average surface energy since its dependence on the orientation of the cleavage plane is not included.

In figure 4, we display the surface energy of [7] for simple metals as a function of the r_s determined in the present work. The correlation is obvious, the dispersion with respect to the average curve being very small. In figure 5, we give the same curves for the 4d and 5d metals. There is no difficulty in determining a curve for each series, and they are very close together. Figure 6 shows that, in the case of the 3d series, it is not possible to find a unique monotonic curve for all the metals. Instead, when one follows the series for increasing Z, γ first increases up to vanadium and then decreases for chromium and manganese; then it reincreases up to cobalt along the same path and then decreases again towards the curve relating to simple metals, but with a trajectory distinct from that corresponding to the first metals of the series, so it is more convenient to speak of a loop rather than of a curve for the 3d series. We can also see that the general trend is similar with γ plotted, in figure 7, versus the r_s^* of Moruzzi, but gives a more open loop. Thus, γ seems to correlate more
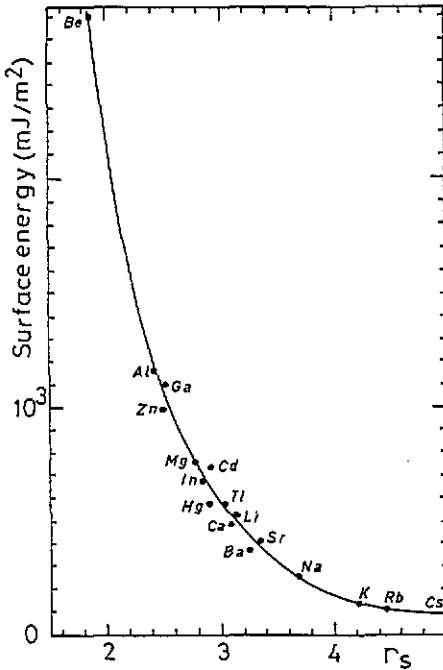
Figure 4. The surface energy versus the effective r_s of this work, for simple metals.
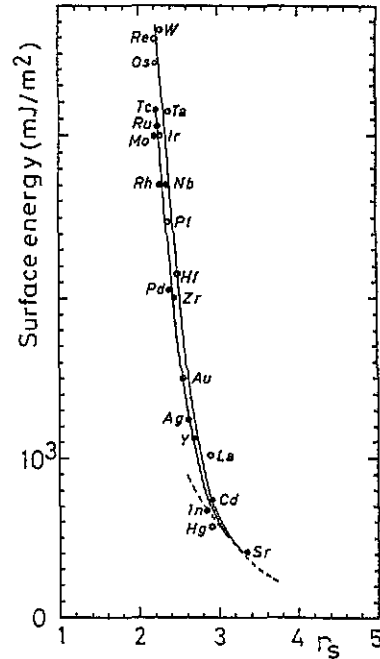
Figure 5. Surface energy of the 4d and 5d transition metals versus the effective r_s of this work: full circles, 4d series, left curve; open circles, 5d series, right curve. The dashed curve corresponds to simple metals.

strongly to the present r_s than to r_s^*. The surface energy of the 3d metals has been analysed recently by Aldén *et al* [11]. These authors have calculated γ, using local spin density theory and a Green function technique based on the linear muffin tin orbital method, and shown that the anomaly for Cr, Mn, Fe and Co is due to a decrease in the d contribution to γ caused by spin polarization [11].

4. Conclusions

We conclude with several more observations. The question may be raised of how sensitive the present results are to the form of the test potential used here. This test potential was chosen in the form of (3) because if indeed our picture of s and p electrons carrying the main response to an external potential with the d electrons remaining largely unpolarized is correct, then to extract the s and p response the test potential should neither introduce additional charge nor have major overlap with the d levels. $V_{sr}(r)$ in (3) satisfies these conditions. The value of r_s should not depend on the test potential $V_{sr}(r)$. We tested this by changing λ in (3) from $\lambda = 1$ to $\lambda = \frac{1}{2}$ and recalculated the case of Cu. The r_s value in this material changed from 2.25 when $\lambda = 1$ to 2.30 when $\lambda = \frac{1}{2}$. This adds considerable confidence that the concept of an effective r_s in these complicated band structures of the transition metal series is indeed meaningful.

In conclusion, we have presented a new list of r_s values for simple and transition metals based on the concept of the metallic response to external low-symmetry perturbations. These
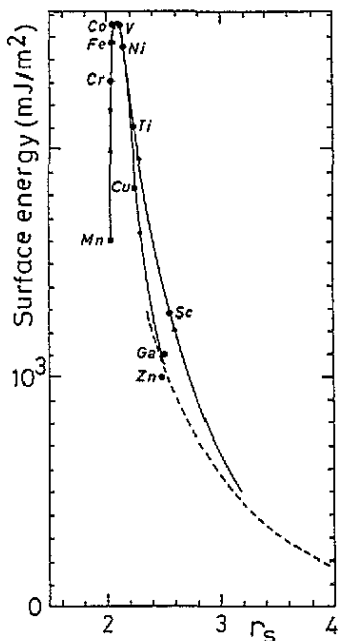
Figure 6. Surface energy of the 3d metals versus the effective r_s of this work. The arrows indicate the progression along the path when the atomic number increases. The dashed curve corresponds to simple metals.
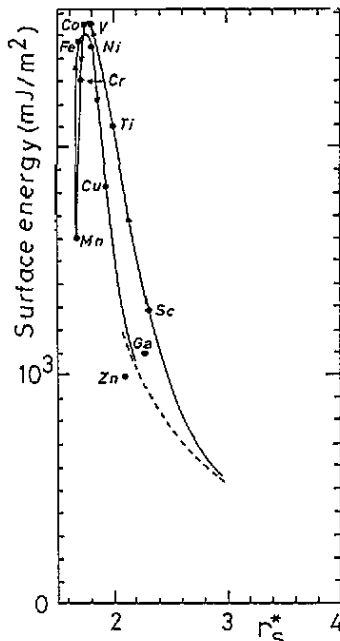
Figure 7. As figure 6, but with the effective r_s^* from the KKR calculations of Moruzzi *et al* [6].

values could serve as a useful starting point in calculating the properties of various defects in these materials.

Acknowledgments

References

[1] Abrikosov A A, Gorkov L P and Dzyaloshinski I E 1963 *Methods of Quantum Field Theory in Statistical Physics* (New York: Prentice-Hall)
[2] Vignale G and Rasolt M 1987 *Phys. Rev. Lett.* **59** 2360
[3] Newns D, Pattnaik P C, Rasolt M and Papaconstantopoulos D A 1988 *Phys. Rev.* B **38** 7033
[4] Kittel C 1986 *Introduction to Solid State Physics* (New York: Wiley)
[5] Ashcroft N W and Mermin N D 1976 *Solid State Physics* (New York: Holt, Rinehart and Winston)
[6] Moruzzi V L, Janak J F and Williams A R 1978 *Calculated Electronic Properties of Metals* (New York: Pergamon)
[7] De Boor F R, Boom R, Mattens W C M, Miedema A R and Niessen A K (eds) 1988 *Cohesion in Metals* (Amsterdam: North-Holland) p 672
[8] Lang N D and Kohn W 1970 *Phys. Rev.* B **1** 4555

[9]   Kohn W and Yaniv A 1979 *Phys. Rev.* B **20** 4948
[10]   March N H and Tosi M P 1984 *Coulomb Liquids* (London: Academic) p 323
[11]   Aldén M, Skriver H L, Mirbt S and Johansson B 1992 *Phys. Rev. Lett.* **69** 2296